

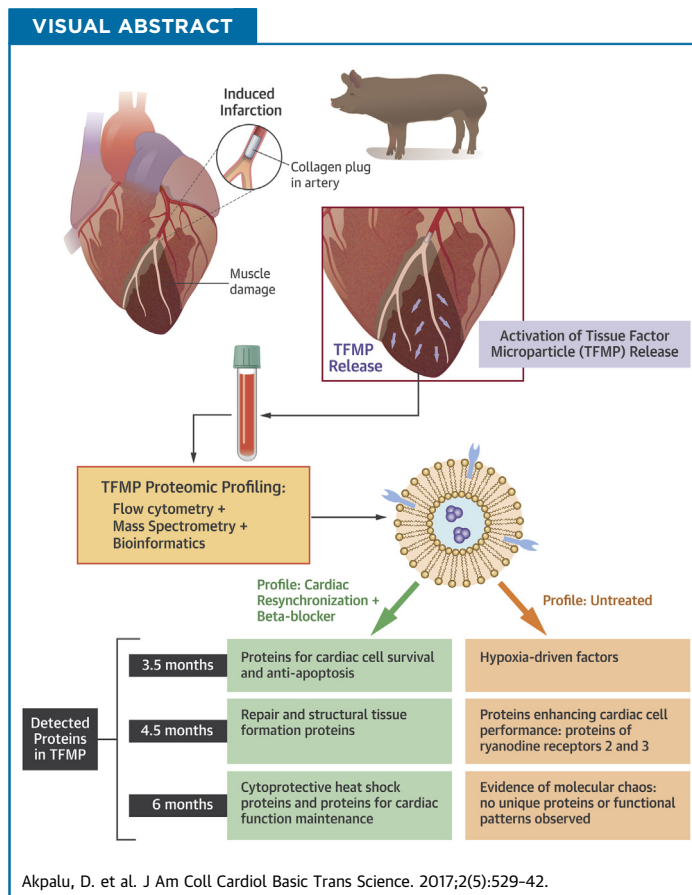
PRECLINICAL RESEARCH

# Matrix Signaling Subsequent to a Myocardial Infarction



## A Proteomic Profile of Tissue Factor Microparticles

Derrick Akpalu,<sup>a</sup> Gale Newman, PhD,<sup>a</sup> Mark Brice, PhD,<sup>a</sup> Mike Powell, PhD,<sup>a</sup> Rajesh Singh, PhD,<sup>a</sup> Alexander Quarshie, MD,<sup>b</sup> Elizabeth Ofili, MD,<sup>b</sup> James Fonger, MD,<sup>c</sup> Nic Chronos, MD,<sup>d</sup> David Feldman, MD, PhD<sup>e,f</sup>



**HIGHLIGHTS**

- The occurrence of an MI activates production of TFMPs.
- We induced an MI in Yucatan miniswine and collected plasma samples over a 6-month period post-MI.
- Experimental groups consisted of infarcted but untreated animals and infarcted animals treated with CRT plus  $\beta$ -blocker.
- Using proteomic profiling, we confirm the heterogeneity of TFMP protein content with respect to physiological status of the host temporally.
- Spatially, the contents of the TFMPs provided information about multiple entities supplemental to what we obtained from assessing a set of 8 currently used cardiac biomarkers.
- The results from this study support recommending TFMP protein content profiling be used prospectively as a viable investigative methodology for chronic ischemic cardiomyopathy to help improve our understanding of  $\beta$ -adrenergic receptor signaling after an MI.

From the <sup>a</sup>Department of Microbiology, Biochemistry and Immunology, Morehouse School of Medicine, Atlanta, Georgia; <sup>b</sup>Clinical Research Center, Morehouse School of Medicine, Atlanta, Georgia; <sup>c</sup>CardioScout LLC, Atlanta, Georgia; <sup>d</sup>Cardiology Care Clinic of Lake Oconee, Eatonton, Georgia; <sup>e</sup>Division of Cardiology University of Cincinnati Medical Center, Cincinnati, Ohio; and the <sup>f</sup>Department of Cardiology, Inselspital Hospital, University of Bern, Switzerland. This work was supported by the following National Institutes of Health (NIH) and National Institute on Minority Health and Health Disparities (NIMHD) grants: NIH 5R01HL84498-5, NIH/NIMHD 2S21MD000101NIMHD 8U54MD007588-04; the Minority Biomedical Research Support of the Research Initiative for Scientific Advancement program 5R25GM058268; the Research Centers in Minority Institutions 5G12MD007602; and NIH/NHLBI contract grant number R21HL092358. All authors have reported that they have no relationships relevant to the contents of this paper to disclose.

## ABBREVIATIONS AND ACRONYMS

**ADRB1** =  $\beta$ 1-adrenergic receptor

**ADRB2** =  $\beta$ 2-adrenergic receptor

**AR** = adrenergic receptor

**ARRB1** =  $\beta$ 1-arrestin

**BB** =  $\beta$ -blocker

**cAMP** = cyclic adenosine monophosphate

**CRT** = cardiac resynchronization therapy

**EDV** = end-diastolic volume

**EF** = ejection fraction

**ELISA** = enzyme-linked immunosorbent assay

**ESV** = end-systolic volume

**FACS** = fluorescence-activated cell sorting

**GRK** = G-protein receptor kinase

**HSP** = heat shock protein

**HUVEC** = human umbilical vein endothelial cell

**LVAd MV** = left ventricular area around the mitral valve at diastole

**LVAs MV** = left ventricular area around the mitral valve at systole

**LVAd PM** = left ventricular area around the papillary muscle at diastole

**LVAs PM** = left ventricular area around the papillary muscle at systole

**MI** = myocardial infarction

**MP** = microparticle

**PCR** = polymerase chain reaction

**TF** = tissue factor

**TFMP** = tissue factor-bearing microparticle

**TnT** = troponin T

## SUMMARY

This study investigated the release and proteomic profile of tissue factor microparticles (TFMPs) prospectively (up to 6 months) following a myocardial infarction (MI) in a chronic porcine model to establish their utility in tracking cellular level activities that predict physiologic outcomes. Our animal groups ( $n = 6$  to  $8$  each) consisted of control, noninfarcted (negative control); infarcted only (positive control); and infarcted animals treated with cardiac resynchronization therapy (CRT) and a  $\beta$ -blocker (BB) (metoprolol succinate). The authors found different protein profiles in TFMPs between the control, infarcted only group, and the CRT + BB treated group with predictive impact on the outward phenotype of pathological remodeling after an MI within and between groups. This novel approach of monitoring cellular level activities by profiling the content of TFMPs has the potential of addressing a shortfall of the current crop of cardiac biomarkers, which is the inability to capture composite molecular changes associated with chronic maladaptive signaling in a spatial and temporal manner. (J Am Coll Cardiol Basic Trans Science 2017;2:529-42) © 2017 Published by Elsevier on behalf of American College of Cardiology Foundation. This is an open access article under the CC BY-NC-ND license (<http://creativecommons.org/licenses/by-nc-nd/4.0/>).

Advances in diagnosis and management of myocardial infarction (MI) have accounted for a decrease in acute mortality from MI (1,2). Much, however, remains to be understood about the cellular and molecular mechanisms of MI longitudinally beyond the initial few days and weeks.

Progressive chronic heart failure and the reduction in cardiac output after an MI cause the activation of neurohormonal responses and perturbation in long-term adrenergic signaling, which leads to changes in the sympathetic nervous system (3).  $\beta$ -adrenergic receptor (AR) activation, in addition to increasing acute cardiac performance, initiates multiple signaling cascades simultaneously through G-protein receptor kinases (GRKs) and  $\beta$ -arrestin-mediated pathways. With an adaptive upregulation of GRK2, there is a concordant increase in heart failure phenotype, in part mediated by the depletion of  $\beta$ -AR-mediated inotropic reserve (4-6). Additionally, chronic activation of the sympathetic nervous system leads to pathological remodeling, necrosis, and apoptosis (7). Two

important aspects in the treatment of chronic heart failure with pathological remodeling include the use of  $\beta$ -blockers (BBs) and cardiac resynchronization therapy (CRT) (4-6). Together these interventions improve

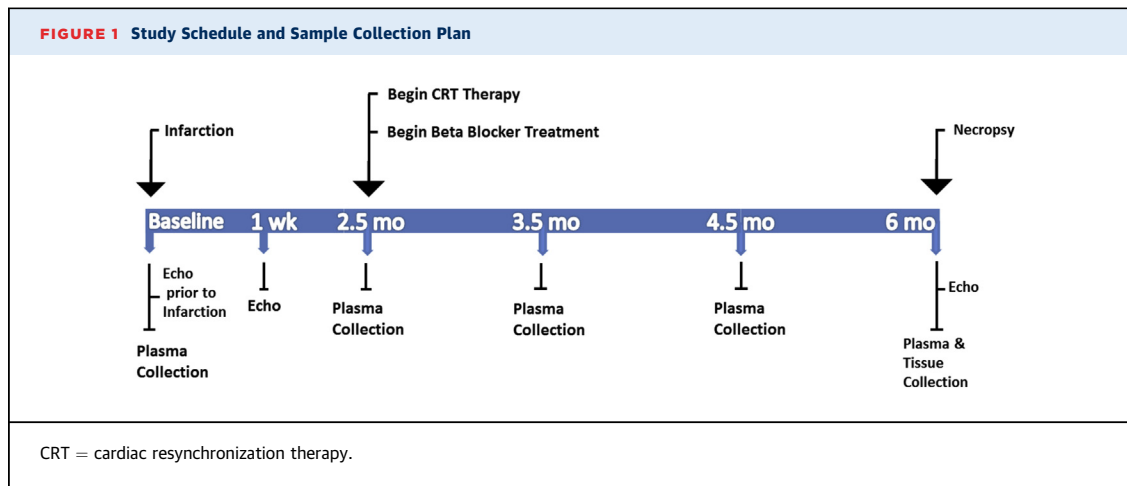
symptoms and enhance left ventricular function while slowing down the progression of maladaptive remodeling and improving morbidity and mortality in appropriately selected patients (4-6).

Previous investigations revealed an elevation of microparticle (MP) levels in patients with cardiovascular diseases, specifically those with acute coronary syndromes (8-11). MPs are small vesicles released from the plasma membrane of cells such as platelets, leukocytes, erythrocytes, endothelial cells, and muscle cells; they contain cell surface proteins along with cytoplasmic components of their cells of origin (8,9,12-15). MPs produced as a result of human atherosclerotic plaque formation possess tissue factor (TF) activity along with an outer membrane composed of phosphatidylserine for prohemostatic activity (8,9,11,12,16,17). In patients with various forms of cardiovascular disease, circulating MPs cause endothelial cell dysfunction (9,11,12,16,18-20) and act as a key driver of atherosclerosis (9,12,13,15,21). In addition to ensuring hemostasis, TF plays a cell signaling role by promoting pleiotropic inflammatory responses. Hitherto, the reports of the elevation of tissue factor (TF) microparticles (MPs) in patients have been of quantitative observations, with no studies describing the protein content of TFMPs over the long term. This study investigated the release and proteomic profile of TFMPs prospectively after an MI in a chronic porcine model.

The majority of the current models of post-MI signaling are in smaller animal models with limited

All authors attest they are in compliance with human studies committees and animal welfare regulations of the authors' institutions and Food and Drug Administration guidelines, including patient consent where appropriate. For more information, visit the *JACC: Basic to Translational Science* [author instructions page](#).

Manuscript received November 17, 2016; revised manuscript received February 27, 2017, accepted April 4, 2017.



duration. For a variety of reasons, investigators typically follow signaling for a few hours to several weeks. Because humans usually do not develop pathological remodeling or heart failure in days or weeks, the purpose of this study was to identify additional mechanisms involved in progressive heart failure over time. An approach that enables the observation of both spatial (membrane to the nucleus) and temporal signaling in a large animal model would enhance our understanding of the multifaceted post-ischemic processes. Investigators have established that signaling pathways seldom function in isolation but are part of a matrix and involve the activation of multiple pathways at different time intervals (22). Hence, we propose that evaluation of discrete signaling pathways for a moment in time might not adequately capture the complex signaling observed in humans.

## METHODS

**ANIMAL MODEL OF MI.** All animal studies were approved by the St. Joseph's Translational Research Institute and Morehouse School of Medicine Institutional Animal Care and Use Committee and comply with The Guide for the Care and Use of Laboratory Animals (8th edition, 2011). The animals were housed individually and had access to food and water ad libitum to exceed all animal standards. Eight-month-old female Yucatan miniswine were infarcted by use of a collagen plug procedure (23). Two and a half months after the infarct, animals were placed in 1 of 2 experimental groups. Pigs in the first group ( $n = 8$ ) had a collagen plug-induced MI and survived but received no treatment, whereas pigs in the second group ( $n = 6$ ) were MI survivors treated with CRT plus a BB (metoprolol). The third group of female control pigs ( $n = 8$ ) had no infarction or treatments. Plasma

was collected at 2.5, 3.5, 4.5, and 6 months after infarction (Figure 1). All infarcted animals were killed at 6 months.

**MI PROCEDURE.** All animals were intubated, and the ear or external jugular vein was cannulated to maintain adequate anesthesia throughout the procedure. The animals (weighing 45 to 55 kg each) were sedated with ketamine combined with xylazine and maintained on isoflurane (0% to 5%). Buprenorphine or morphine was given perioperatively. Arterial pressure was monitored by accessing a femoral artery with an appropriately sized vascular introducer sheath. Heparin (150 U/kg) was administered, and 10 to 30 min later, activated clotting time was checked to confirm it was  $>300$  s. An appropriately sized guiding catheter was introduced and advanced to the ostium of the left main coronary artery, and contrast angiography was performed. An infusion catheter was advanced through the guiding catheter into the midportion of the left anterior descending coronary artery. At the discretion of the operator,  $\approx 2$  ml of collagen was injected in 0.2-ml increments to occlude the majority of the left anterior descending coronary artery. Additional buprenorphine was given for immediate post-operative analgesia 1 to 2 times per day for 1 to 5 days after infarction.

**CRT AND BB THERAPY.** Biventricular pacing devices were implanted as described previously (24). Briefly, pigs that had an MI were treated with CRT and BB therapy (metoprolol succinate, Novartis, Basel, Switzerland) titrated to 2 mg/kg over several weeks, from 2.5 months post-infarction until termination at 6 months. This dosing was intended to emulate the dosing used in MERIT-HF (Metoprolol CR/XL Randomized Intervention Trial in Congestive Heart Failure) (25). To achieve a biventricular capture rate  $>95\%$ , pacing was obtained by simultaneous left

lateral wall (via coronary sinus) and right ventricular septal wall pacing. Placement was ensured by fluoroscopy at the time of placement, and fluoroscopy was used at post-operative 3 days and at 1 month to ensure capture.

**BLOOD SAMPLE COLLECTION, STORAGE, AND NECROPSY.** Blood samples (7 to 8 ml) were collected into ethylenediaminetetraacetic acid tubes (BD Vacutainer Systems, Franklin Lakes, New Jersey). The plasma samples were centrifuged at  $2,000 \times g$  (20 min) to remove any residual platelets, cell debris, and precipitates. Platelet-poor plasma was stored frozen at  $-80^{\circ}\text{C}$  in 1-ml aliquots until one-time use at analysis. Plasma samples were subjected to no further freeze-thaw cycles.

**QUANTITATION ASSAYS (HIGH-SENSITIVITY TROPONIN T,  $\beta$ 1-AR,  $\beta$ 2-AR,  $\beta$ -ARRESTIN-1, cAMP, EPINEPHRINE, NOREPINEPHRINE, AND GRK2).** To measure  $\beta$ 1-AR (ADRB1),  $\beta$ 2-AR (ADRB2),  $\beta$ 1-arrestin (ARRB1), and cyclic adenosine monophosphate (cAMP) levels, porcine hearts were harvested when the animals were killed 6 months after the infarction. Harvested cardiac tissue was rinsed with phosphate-buffered saline and quickly frozen in liquid nitrogen. Frozen tissue was then placed in RNeasy RNA Stabilization Reagent (Qiagen, Valencia, California) and stored at  $-80^{\circ}\text{C}$ . Frozen ventricle samples were homogenized in protein lysate buffer before being centrifuged for 20 min at 2,000 rpm. The supernatant was assayed for ARRB1, ADRB1, ADRB2, and cAMP content by enzyme-linked immunosorbent assay (ELISA) (MyBioSource Inc., San Diego, California) in accordance with the manufacturer's protocol. Real-time polymerase chain reaction (PCR) was used to measure levels of GRK2 (Qiagen OneStep real-time PCR and HotStarTaq Plus Master Mix kit). Harvested cardiac tissue samples were analyzed for fibrosis intensity using a commercially available trichrome stain (Masson) kit following the assay procedure detailed by Sigma-Aldrich (St. Louis, Missouri).

Plasma samples were collected and used to determine the levels of troponin T (TnT) by ELISA (Life Sciences Advanced Technologies, Inc., St. Petersburg, Florida) following the manufacturer's protocol. Concentrations of epinephrine and norepinephrine were determined with plasma samples by ELISA at all 4 time points post-infarction. (MyBioSource Inc.).

**MP ISOLATION AND LABELING.** Platelet-poor plasma was centrifuged at  $20,000 \times g$  (30 min) to pellet the MPs. The MP pellet was washed by resuspension in Hank's balanced salt solution (Sigma-Aldrich). The washed pellet was incubated in 200  $\mu\text{l}$  of binding buffer with saturating concentrations (20  $\mu\text{l}$ ) of

fluorescein isothiocyanate-conjugated annexin V antibody (Clontech, Mountain View, California) and phycoerythrin-conjugated TF antibody (Abcam, Cambridge, Massachusetts) for 1 h on ice in the dark. After labeling, the MPs were washed by resuspension with Hank's balanced salt solution to remove excess unbound antibody by pelleting at  $20,000 \times g$  for 30 min and resuspending in 500  $\mu\text{l}$  of Hank's solution before fluorescence-activated cell sorting (FACS) analysis.

**FLOW CYTOMETRY SORTING OF MPs.** Analysis of TFMPs was performed with 2-color flow cytometry on a BD FACS Aria II equipped with the FACS DIVA software, version 6.1.2 (BD Biosciences, San Jose, California). The MPs were analyzed with logarithmic measurements for forward scatter and side scatter. TFMPs were sorted based on double positivity for TF antigen and annexin V, which identifies TFMPs. The sorted TFMPs were centrifuged at  $100,000 \times g$  to recover all MPs in the sample for proteomic analysis.

**MASS SPECTROMETRY ANALYSIS.** The samples were acetone precipitated, rehydrated in trypsin digest buffer (50 mmol/l ammonium bicarbonate), reduced in dithiothreitol 10 mmol/l at  $56^{\circ}\text{C}$  for 30 min, and alkylated with iodoacetic acid (15 mmol/l) for 30 min at room temperature in the dark. Samples were trypsin digested 20 (ng/ $\mu\text{l}$ ) for 4 h at  $37^{\circ}\text{C}$ , and before analysis, they were acidified by formic acid to a concentration of 0.1%. Spectra were collected with Xcalibur 2.2 software (Thermo Fisher Scientific, Waltham, Massachusetts) using a threshold of 200 counts/hits. Spectra were then searched with Proteome Discoverer 3.0 software (Thermo Fisher Scientific). Each sample produced 1 or 2 significant hits as determined by false discovery rates of 1.0% and 5.0% using a corresponding reverse database.

Porcine peptide sequences detected were exported from ProteoIQ software version 2.3.08 (NuSep, Inc., Bogart, Georgia) into protein BLAST, Blastp (National Center for Biotechnology Information) and were checked against the human protein database to determine porcine/human protein homologs. Only human proteins with  $>85\%$  homology were used for the analysis. This conversion was necessary because Pathway Studio (Elsevier, Atlanta, Georgia) only uses proteins from humans, mice, and rats in its analysis. The resultant homologous human protein Entrez ID numbers were uploaded into Pathway Studio 10 for pathway analysis.

**PATHWAY AND FUNCTIONAL ENRICHMENT ANALYSIS.** Pathway Studio version 10 (PS10) with Disease Fx and Chem Fx cartridges was used to analyze the proteomic data between the different treatment groups and an analysis of cell processes, disease processes, and

functional classes determined for the identified proteins. Functional enrichment analysis was conducted with FunRich (26) version 2.1.2 (27).

**STATISTICAL ANALYSIS.** SigmaPlot version 12 was used for the statistical analysis of MP counts, ELISA, and PCR data. Where nonparametric methods of analysis were applied, data are summarized using median (1st quartile, 3rd quartile); otherwise data are expressed as mean  $\pm$  SD. Comparisons were made using nonparametric tests, Kruskal-Wallis 1-way analysis of variance and Mann-Whitney rank sum test, as appropriate. Dunn's method was applied to the probability values whenever multiple comparisons arose. To compare TFMP count changes across time within treatments groups, the Wilcoxon matched-pairs signed ranks method was applied. The 1-way repeated-measures analysis of variance method was applied to the TnT data with multiple pairwise comparison involving the Holm-Sidak method applied. All tests were 2-sided, with  $p < 0.05$  considered significant.

## RESULTS

**HEMODYNAMIC, CARDIAC DIMENSION, AND FIBROSIS INTENSITY OBSERVATIONS.** Assessments of end-diastolic volume (EDV), end-systolic volume (ESV), and ejection fraction (EF) were made at baseline, 1 week post-infarction, and at study termination. Overall, after the MI, there were increases in EDV and ESV with decreasing EF in both infarcted groups of animals. There were no statistically significant differences between groups at baseline or at 1 week post-infarction. Baseline EDVs for the CRT+BB-treated animals and for infarcted, untreated animals averaged  $49.25 \pm 20.47$  ml and  $53.10 \pm 15.67$  ml, respectively ( $p = 0.722$ ). Median ESV values for the treated versus untreated animals were 17.86 ml (15.35 ml, 21.223 ml) and 20.47 ml (12.49 ml, 25.43 ml), respectively ( $p = 0.931$ ). Baseline EF for CRT+BB-treated versus infarcted, untreated animals averaged  $59.78 \pm 5.32\%$  and  $61.85 \pm 2.52\%$ , respectively ( $p = 0.448$ ).

Post-infarction EDV values for CRT+BB-treated versus infarcted, untreated animals averaged  $73.61 \pm 14.60$  ml and  $85.86 \pm 16.67$  ml, respectively ( $p = 0.205$ ). At the same time point, ESV values for CRT+BB-treated versus infarcted, untreated animals averaged  $50.67 \pm 11.96$  ml versus  $56.93 \pm 9.88$  ml, respectively ( $p = 0.375$ ). The assessed EF for the CRT+BB-treated and infarcted, untreated groups after infarction averaged  $27.22 \pm 5.18\%$  and  $24.15 \pm 1.44\%$ , respectively ( $p = 0.238$ ).

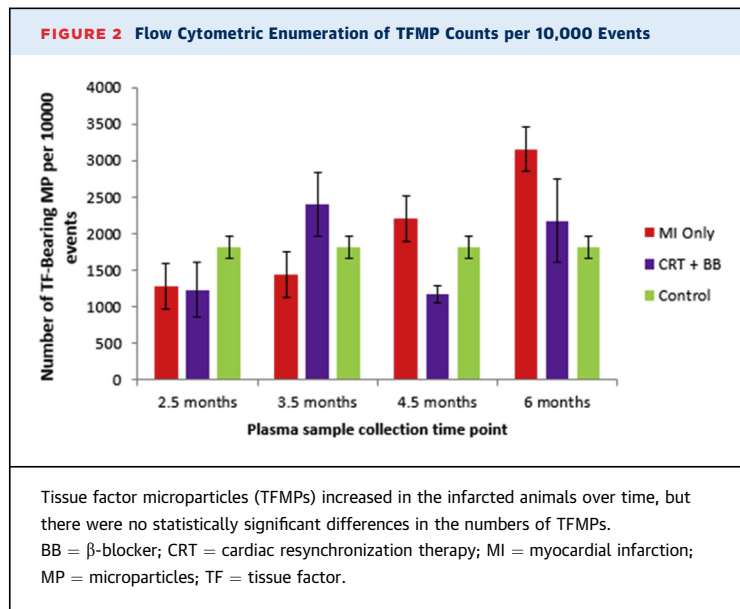
At termination of the study, there was a statistically significant difference ( $p = 0.046$ ) in mean EDV

values between the 2 infarcted groups (CRT+BB  $112 \pm 35.35$  ml vs. MI only  $151.03 \pm 13.14$  ml). At the same time point, there was a noticeable trend of increasing ESV in both groups; however, the increase in ESV values was comparatively more pronounced in the untreated group than in the CRT+BB-treated animals. ESV values for the CRT+BB versus MI-only animals at this time point were  $70.78 \pm 28.03$  ml versus  $104.63 \pm 18.95$  ml ( $p = 0.069$ ). At study termination, EF values for the CRT+BB-treated animals were relatively better than for the infarcted, untreated animals, with the difference approaching statistical significance ( $p = 0.0527$ ) 3.5 months after treatment was initiated in the treatment group. The values were  $37.905 \pm 6.036\%$  versus  $30.865 \pm 5.874\%$  for the CRT+BB and MI-only groups, respectively.

Cardiac dimension measurements were conducted with echocardiograms at baseline, 1 week post-infarction, and after necropsy. Predictably, after the infarction, there was a noticeable increase in cardiac dimensions for all animals, as observed in left ventricular area around the mitral valve at diastole (LVAd MV) and systole (LVAs MV). Additionally, cardiac enlargement was observed in the area around the papillary muscle at diastole (LVAd PM) and systole (LVAs PM). In all groups, there was an increase in these cardiac measurements between the 1-week post-infarction assessment time point and study termination. Comparison of the cardiac dimensions between the 2 infarcted groups at study termination showed no statistical differences with respect to LVAd MV, LVAs MV, and LVAs PM; however, there was a statistically significant difference ( $p = 0.009$ ) in LVAd PM values between the CRT+BB-treated versus MI-only groups.

Extent of fibrosis in the harvested infarcted hearts was also determined on a scale of 1 to 4 (0 = normal, 1 = minimal, 2 = mild, 3 = moderate, and 4 = severe), normalized to samples from normal, uninfarcted porcine hearts. Seven cardiac regions were examined: right ventricle lateral wall; septum; border; infarct; normal; left atrium; and right atrium. Briefly, the results revealed grade 3 to 4 fibrosis in the septum, border, and infarct regions of the hearts of both infarcted animal groups. In the right lateral wall, left atrium, and right atrial regions of the harvested cardiac tissues, normal to mild fibrosis was observed.

**TFMP COUNTS.** At 2.5 months post-infarction, there was no significant difference in TFMP counts between the experimental groups (Figure 2). The average TFMP counts per 10,000 events at 2.5 months were  $1,806 \pm 423$  for the control group,  $1,281 \pm 909$  for the infarcted, untreated pigs, and  $1,233 \pm 752$  for the CRT+BB-treated group. Over the remaining time points, the counts of the infarcted, untreated animals



continued to increase to  $3,156 \pm 1,360$ , whereas the counts of the treated animals tracked between  $1,233 \pm 752$  and  $2,173 \pm 1,405$ . Statistically, there were no significant differences in the numbers of MPs within or between the groups at any time points.

**TFMP PROTEOMIC PROFILE.** Mass spectrometry results showed that the proteomic content of TFMPs changed over time within and between groups. For the CRT+BB-treated animals, there were 177, 125, and 137 proteins detected in the TFMPs collected at the 3.5-, 4.5-, and 6-month time points, respectively. In the infarcted, untreated group, we observed 196, 207, and 65 proteins at the 3.5-, 4.5-, and 6-month time points, respectively. The control group animals had 202 different proteins detected at the single time point assessed. The differences and similarities of the proteomic profiles were evaluated for functional enrichment using the FunRich tool and the Pathway Studio software as further described in “Molecular Function Analyses of TFMP proteins.”

On the basis of the sites of expression of the identified proteins, TFMPs were determined to be from heart muscle, plasma, blood vessels, and human umbilical vein endothelial cells (HUVECs), as shown in [Table 1](#). The observed high number of proteins mapped to HUVECs is a consequence of the abundance of model systems involving HUVECs for the identification of endothelial cell function in published literature (28-30). FunRich and other molecular analysis tools rely on published literature for the generation of their output. This observation, however, points to the relevance of these molecular entities in the post-MI state.

#### MOLECULAR FUNCTION ANALYSES OF TFMP PROTEINS.

To further characterize the identified TFMP proteins and to explore for temporal differences, the standalone open-access tool FunRich and Pathway Studios version 10 software were jointly used to determine their molecular functions. Compared with the other 2 groups, the CRT+BB-treated group at the 3.5-month time point had a 6-fold increase in the number of proteins associated with ATPase activity and a lower percentage of proteins functioning as extracellular matrix structural constituent ([Figure 3](#)). The control group had 2.5 times and 4 times as many proteins related to ubiquitin-specific protease activity as did the infarcted, untreated animals and the CRT+BB-treated animals, respectively. With regard to G-protein-coupled receptor activity at the 3.5-month time point, the infarcted, untreated group had the most activity, with nearly a 10- and 5-fold increase in the number of proteins compared with the control and CRT+BB-treated animals, respectively.

At the 4.5-month time point, the TFMP proteins differed in 3 main functional classes between the experimental groups: structural constituents of the cytoskeleton, ATPase activity, and intracellular ligand-gated ion channel activity ([Figure 4](#)). There was a considerable difference in the structural constituents of the cytoskeleton between the CRT+BB-treated animals and the control animals, in the ratio of  $\approx 1:35$  ([Figure 4](#)). The infarcted, untreated animals had no detectable proteins functioning as structural constituents of the cytoskeleton. With regard to ATPase activity, the CRT+BB group recorded the highest percentage, with nearly a 2-fold increase compared to the control group and  $\approx 1.5$  times the number observed in the infarcted, untreated group. The CRT+BB group had no detectable proteins functioning in intracellular ligand-gated ion channel activity, but there was a 4-fold increase in the infarcted, untreated group compared with the control group.

By the 6-month time point, CRT+BB treatment was associated with an  $\approx 4$ -fold increase in ATPase protein content compared with controls, whereas the infarcted, untreated animals had 3 times as many ATPase proteins as the control animals. There were no proteins associated with extracellular ligand-gated ion channel activity detected in the CRT+BB group, although in the infarcted, untreated animals, there was a 3-fold increase compared with the control group. The infarcted animals had higher levels of extracellular matrix structural constituents than the control group animals ([Figure 5](#)). Additionally, the infarcted, untreated animals had a higher percentage of proteins associated with ubiquitin protease activity than the

CRT+BB-treated group (1:8 ratio) and an ≈50% increase compared with the control group animals.

**TFMP PROTEIN CONTENT AND POST-MI DISEASE STATUS.**

To further understand the association between disease status and TFMP protein content, Pathway Studio analysis was conducted. Evaluations were based on functional associations with known active cell processes post-MI, such as apoptosis, oxidative stress, and inflammation, with adjustments made for the administration of the BB metoprolol where applicable.

At the 3.5-month time point (Supplemental Figure 1), TFMP proteins in the treated group were associated with cardiac cell antiapoptosis and facilitation of cardiomyocyte function. These TFMP proteins included sarcoplasmic/endoplasmic reticulum Ca<sup>2+</sup>-ATPase, SERCA proteins (ATP2A2), ephrin, and hexokinase 1 and 2 (HK I, HK II). Another cardiac cell-enhancing factor detected in the treated group but not the infarcted, untreated group or control group was guanylate cyclase A. Conversely, at the 3.5-month time point, hypoxia-driven factors such as hypoxia-inducible factor-1 $\alpha$ , hypoxia-inducible factor-2 $\alpha$ , and FLT-1 (Fms-related tyrosine kinase-1) were detected in the infarcted, untreated animals.

At the 4.5-month time point, repair and structural tissue formation proteins were found in the CRT+BB-treated group (Supplemental Figure 2). These proteins were keratin, desmin, actin, vimentin, myosin, and  $\beta$ -catenin. Compared with the treated pigs, there were fewer myosin subtypes observed in the infarcted, untreated group. Additionally, proteins that enhance cardiac cell performance, such as sodium/potassium-transporting ATPase subunit alpha-1 and -2 (ATP1A1, ATP1A2), and proteins of ryanodine receptors 2 and 3 (RYR2, RYR3) were observed in the untreated group. Furthermore, in both infarcted groups, factors that can promote inflammation were detected; however, in addition to thrombin (F2), TF, and putative serine proteases (PRSS), which were detected in the treated group, nuclear factor-kappa-B1 (NF-KB1) and ADAM metallopeptidase domain 17 (ADAM17) were detected in the infarcted, untreated group.

By the 6-month time point, TFMPs in the treated group contained cytoprotective heat shock proteins (HSPs) such as HSPA1A, HSPA1B, and HSPA5 (Figure 6). HSP was not detected in any other group. In addition to the cytoprotective proteins, pigs in the treated group contained proteins required for the maintenance of cardiac function (ATP1A1 and ATP1A2). There were no unique proteins or functional patterns observed in the infarcted, untreated animals at this time point.

**HIGH-SENSITIVITY CARDIAC TnT ASSESSMENT.** Serum levels of TnT were assessed between groups (Figure 7). Area under the curve analyses for the period from

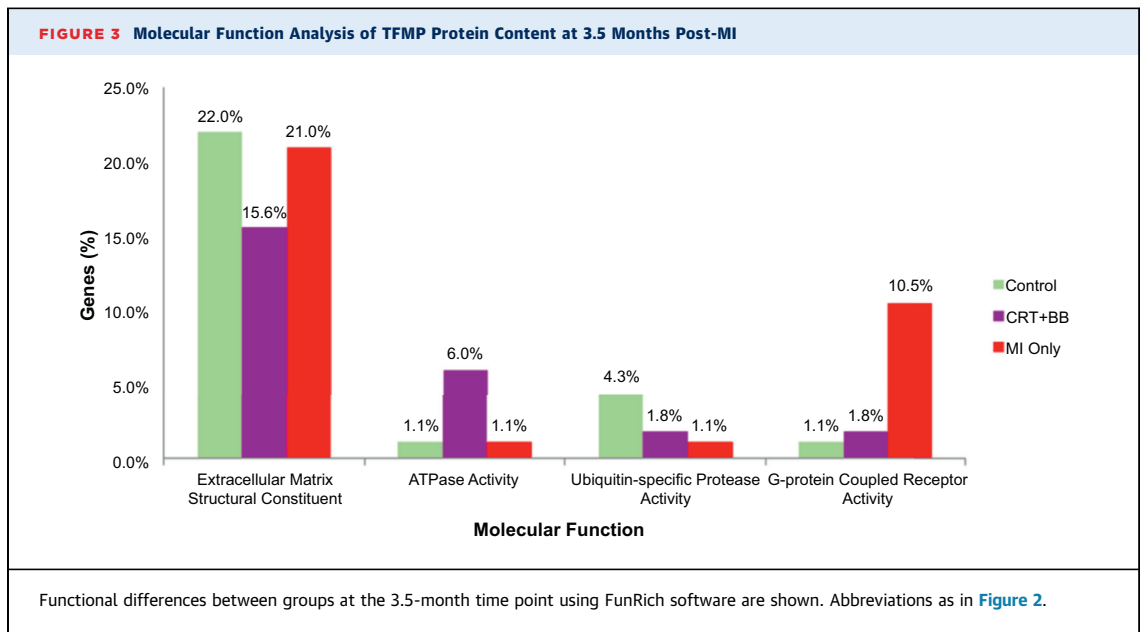
**TABLE 1 FunRich Analysis of Site of Expression of TFMP Protein**

Treatment and Site of Expression	No. of Genes in Dataset	Uncorrected p Value (Hypergeometric Test)	Storey and Tibshirani Method q Value
<b>Control</b>			
Heart muscle	72	0.15	0.07
Plasma	156	0.00	0.00
Blood vessels	8	0.00	0.00
HUVECs	163	0.00	0.00
<b>Untreated 3.5 months</b>			
Heart muscle	77	0.01	0.00
Plasma	138	0.00	0.00
Blood vessels	10	0.00	0.00
HUVECs	143	0.01	0.00
<b>Untreated 4.5 months</b>			
Heart muscle	76	0.13	0.09
Plasma	158	0.00	0.00
Blood vessels	7	0.00	0.00
HUVECs	172	0.00	0.00
<b>Untreated 6 months</b>			
Heart muscle	29	0.03	0.09
Plasma	52	0.00	0.02
Blood vessels	2	0.07	0.12
HUVECs	52	0.03	0.09
<b>CRT+BB 3.5 months</b>			
Heart muscle	62	0.20	0.09
Plasma	142	0.00	0.00
Blood vessels	9	0.00	0.00
HUVECs	141	0.00	0.00
<b>CRT+BB 4.5 months</b>			
Heart muscle	50	0.04	0.01
Plasma	106	0.00	0.00
Blood vessels	1	0.58	0.07
HUVECs	98	0.00	0.00
<b>CRT+BB 6 months</b>			
Heart muscle	51	0.09	0.01
Plasma	112	0.00	0.00
Blood vessels	8	0.00	0.00
HUVECs	109	0.00	0.00

BB =  $\beta$ -blocker; CRT = cardiac resynchronization therapy; HUVECs = human umbilical vein endothelial cells; TFMP = tissue factor-bearing microparticles.

2.5 to 6 months post-MI were conducted. ANOVA was highly statistically significant across all comparisons: MI versus control,  $p < 0.001$ ; MI versus CRT+BB,  $p < 0.002$ ; and CRT+BB versus control,  $p < 0.002$ .

**ADRB2, cAMP, AND GRK2 CONCENTRATIONS.** The mean concentration of ADRB2 in myocardial tissue in the control group animals was  $0.681 \pm 0.056$  ng/ml compared to  $0.205 \pm 0.086$  ng/ml in the infarcted, untreated group and  $0.22 \pm 0.223$  ng/ml in the CRT+BB-treated group (Supplemental Figure 3). Statistically, there were differences in the average concentration between the infarcted but untreated group and the control group ( $p = 0.003$ ) and between the CRT+BB-treated group and the control group



( $p = 0.003$ ). There were no statistically significant differences between the infarcted, untreated group and the treated group. Median cAMP tissue concentration for the treated group was  $29.778 \mu\text{g/ml}$  compared with  $17.174 \mu\text{g/ml}$  in the infarcted group ([Supplemental Figure 4](#)), which was statistically significantly different from the control group (CRT+BB vs. control:  $p = 0.05$ ; MI vs. control:  $p = 0.05$ ). GRK2 concentrations using quantitative PCR analysis ([Supplemental Figure 5](#)) from the myocardial tissue at study

termination showed a statistically significant difference ( $p = 0.013$ ) between the treated and untreated animals ( $0.471 \pm 0.349$  RFU/18S [relative fluorescence units/18S ribosomal RNA] and  $1.321 \pm 0.455$  RFU/18S, respectively).

**ADRB1, ARRB1, EPINEPHRINE, AND NOREPINEPHRINE CONCENTRATIONS POST-INFARCTION.** ADRB1 concentrations in cardiac tissue at 6 months after infarction showed levels as follows: treated group > control group > infarcted, untreated group, with mean

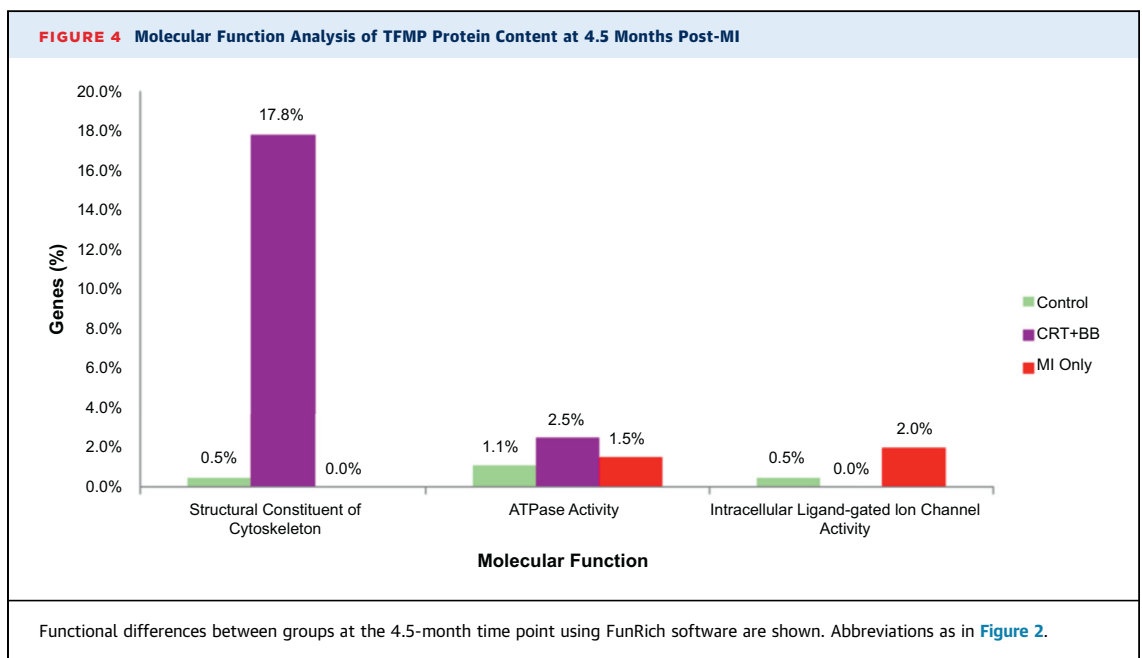
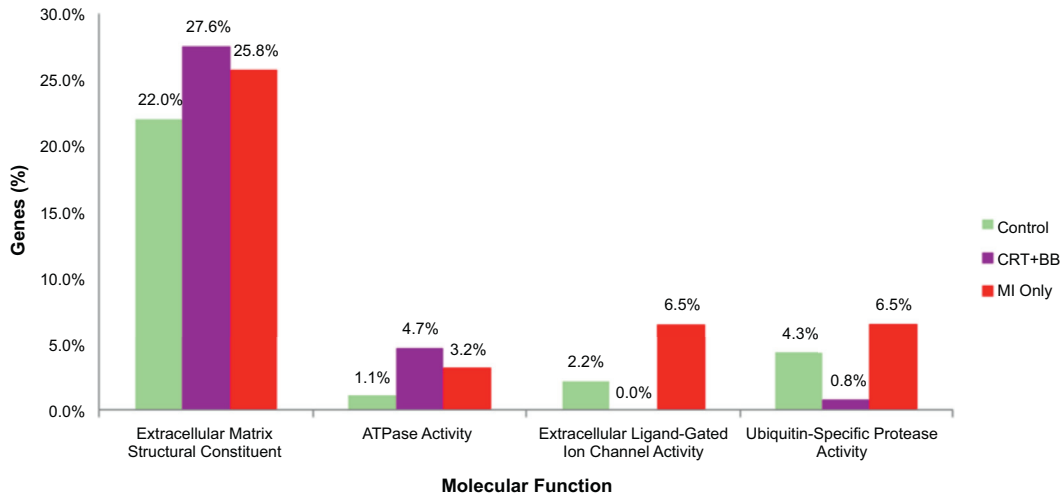
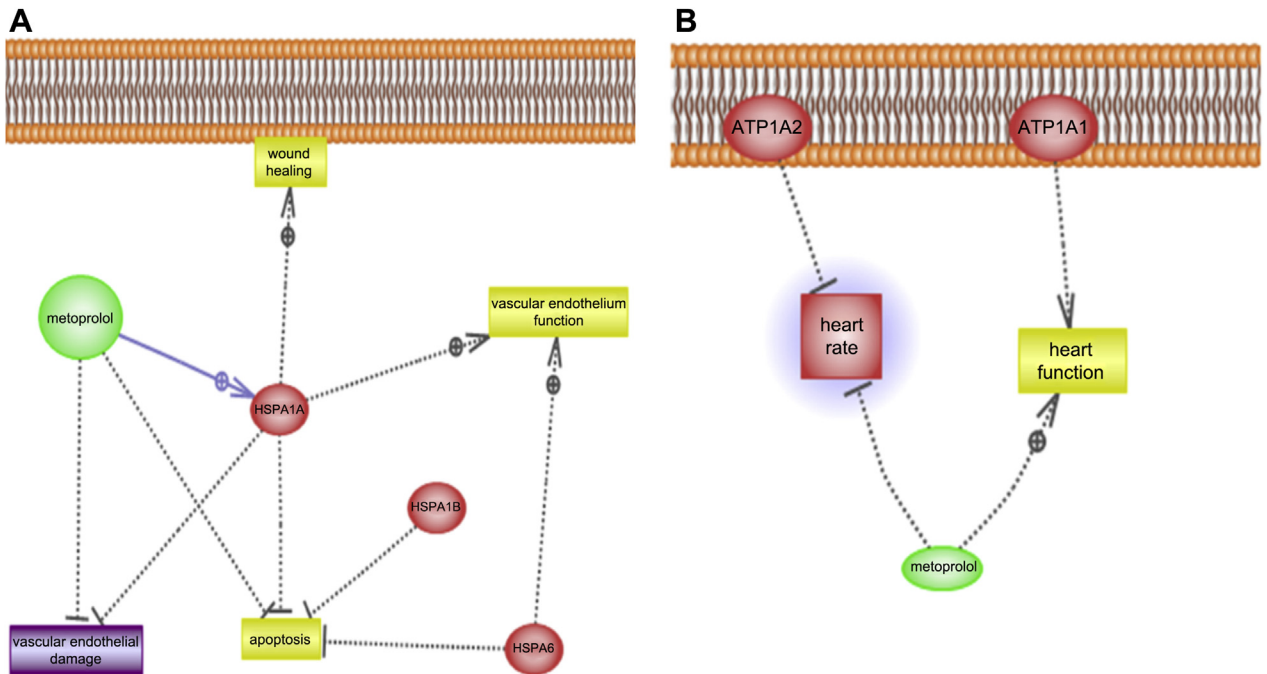


**FIGURE 5 Molecular Function Analysis of TFMP Protein Content at 6 Months Post-MI**



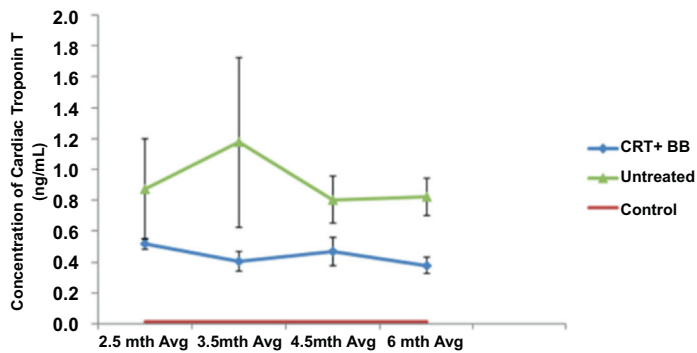
Functional differences between groups at the 6-month time point using FunRich software are shown. Abbreviations as in Figure 2.

**FIGURE 6 Pathway Studio Analysis of Proteomic Content of TFMPs at 6 Months in the Infarcted Groups Compared With Control Group Profile**



**(A)** Heat shock proteins (HSPs) associated with post-ischemic conditioning detected in CRT+BB-treated animals only. Metoprolol administration enhanced levels of HSPA1A. **(B)** Factors related to cardiac function improvement were detected in treated animals 6 months after infarction, but no such observation made in the infarcted, untreated animals.

**FIGURE 7** Serum Troponin T Levels Over the 6-Month Period Post-Infarction Showing Chronic Myocardial Cell Death in Infarcted Animals Over the 6-Month Study Duration



The differences in mean values between the infarcted groups became statistically significant at the 6-month time point ( $p = 0.008$ ). Avg = average; mth = month; other abbreviations as in [Figure 2](#).

concentrations of 0.133 ng/ml, 0.027 ng/ml, and below limits of detection, respectively. There were no significant differences in the mean concentrations of  $\text{ARRB1}$ , epinephrine, and norepinephrine between the experimental groups in our study; however, there was the expected elevation in norepinephrine and epinephrine concentrations in the infarcted animals compared with the control group at all time points.

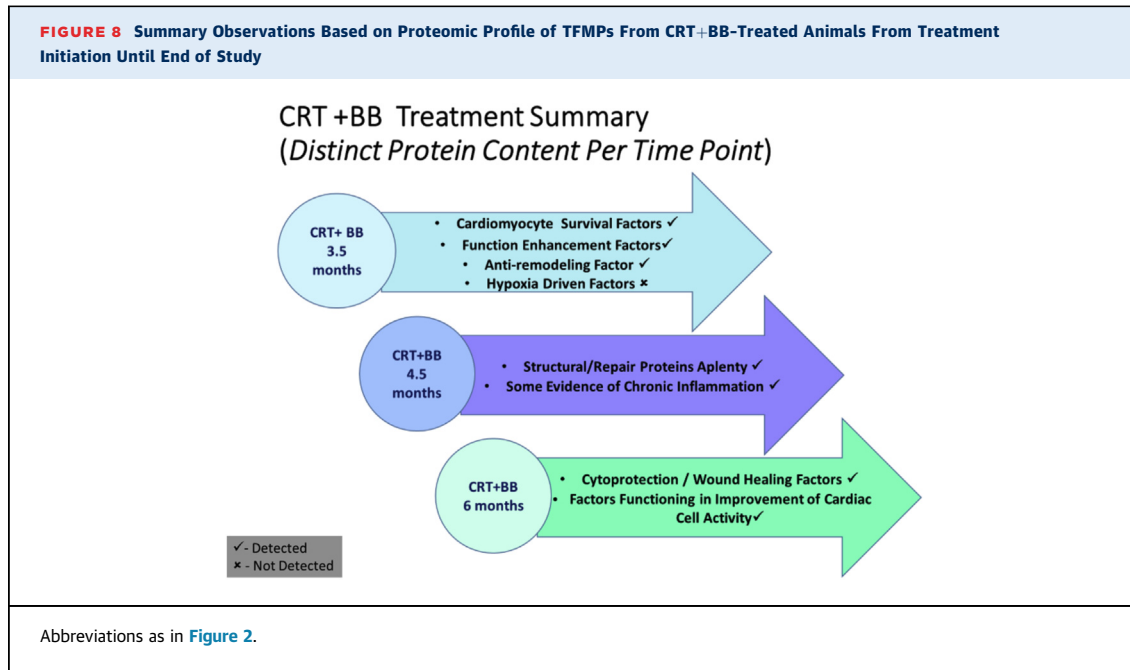
## DISCUSSION

In heart failure patients with severe systolic dysfunction and asynchronous contraction, CRT is an established, effective adjunctive therapy when paired with BB. To adequately emulate the human condition, we used an animal model with decreased EF and asynchrony. The CRT+BB regimen improves left ventricular function and prognosis, whereas metoprolol reduces infarct size (31,32). What is not fully characterized is the long-term signaling impact of  $\beta_1$ -adrenergic blockade on the infarcted heart.

Reports indicate that many of the cellular responses after an MI, such as fibrous tissue deposition, occur within the first few days to weeks of the post-infarction period (33-35). The degree of fibrosis (grade 3 or 4) observed in the septal area, border, and infarct regions of the hearts of both groups of infarcted pigs was in line with the expectation of structural changes (fibrous tissue deposition) reported previously (36). Additionally, the morphological changes in cardiac dimensions showed that this study also depicted the expected morphological alterations observed in clinical settings (37) and

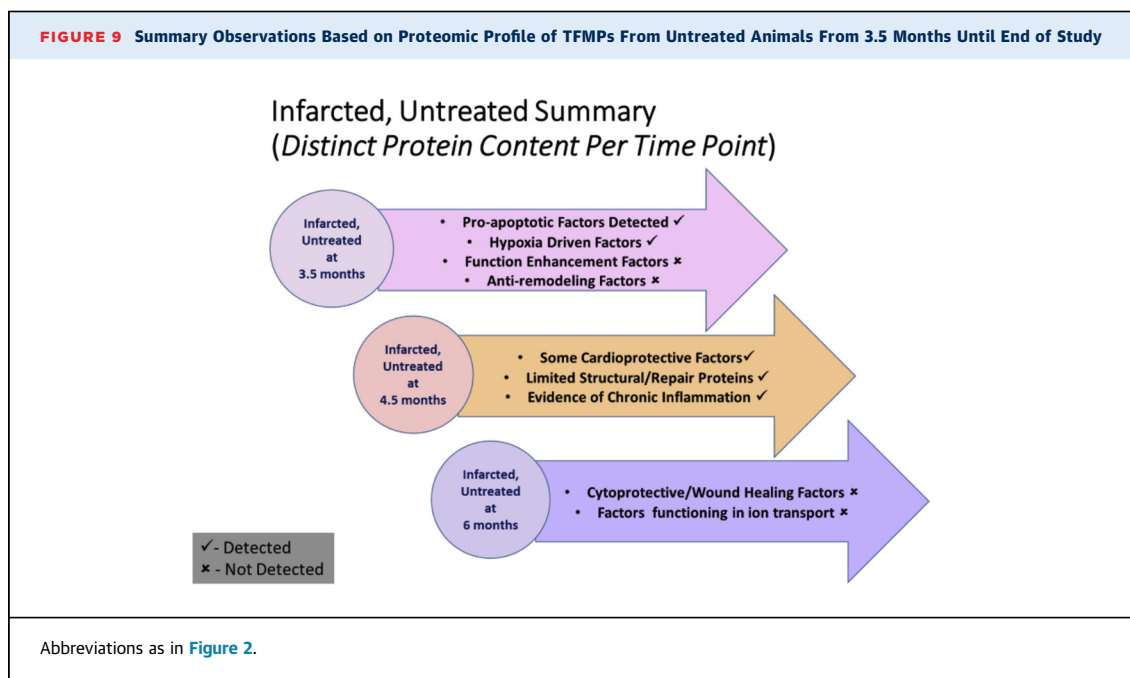
confirmed that the experimental procedure successfully induced the MI and mimicked post-MI observations. Furthermore, the hematologic observations depicted the functional consequences of infarction, as well as treatment, with respect to time. Collectively, the structural, morphological, and function alterations observed are evidence of pathological remodeling in response to infarction. Clinically, the observation of improved EF and the differences in EDV and ESV between the infarcted animals point to a trend toward better outcomes in our treatment group animals than in the infarcted, untreated animals. This observation is in line with general clinical observations of better prognosis with treatment with CRT+BB and also aligns with the observed decline in TnT levels with treatment in our study. Results from this study therefore confirmed the documented beneficial effects of  $\beta_1$  blockade in improving outcomes (31,32). More importantly, the proteomic profile of the TFMPs provided insights into the long-term impact of metoprolol usage on active signaling entities of the surviving cardiomyocytes. First, the inability to differentiate experimental groups in the long-term post-MI stage using TFMP numbers confirmed our view that the more relevant information is the proteomic profile of the TFMPs. Second, our findings demonstrate unique signatures for each infarcted pig cohort associated with either adaptive or healing changes, as well as progressive pathological remodeling or maladaptive signaling leading to worsening heart failure. Additionally, the proteomic profile of the TFMPs provided a matrix view of the spatial and temporal changes and differences in signaling entities between the study groups. We infer from our TFMP proteomic data and Pathway Studio analyses that the improved prognosis of the CRT+BB-treated animals proceeded in a stagewise manner via the following general modalities: 1) cardiomyocyte survival and function enhancement; 2) structural repair; and 3) cytoprotection and post-ischemic conditioning (Figures 8 and 9).

A month after treatment initiation, cardiomyocyte survival and function enhancing factors were detected as depicted by [Supplemental Figure 1A](#). Collectively, the listed proteins confer protective properties to the myocardium by promoting chemomechanical and antiapoptotic properties (38) while attenuating chronic cardiac remodeling (39-41). The detection of SERCA proteins in the CRT+BB-treated group is important, because metoprolol has been reported to restore cellular levels of SERCA2a (42,43). The detection of cardiomyocyte survival factors perhaps explains the trend toward the decrease in levels of TnT in the treated group compared with the infarcted,



untreated animals. In the absence of treatment, the detection of hypoxia-driven factors (Supplemental Figure 1B) predicted worse outcomes for the infarcted, untreated animals, as confirmed by the results of the currently used biomarkers. At stage 2 (2 months after treatment initiation), a wide range of structural or repair proteins were present in the TFMPs of the treated group (Supplemental Figure 2).

This was in contrast to the observed narrower array of structural proteins detected in the infarcted, untreated group. Additionally, the differences in the structural proteins and the late detection of chemomechanical proteins could be evidence of delayed and perhaps ineffective cellular signaling in the absence of treatment. The observed wide range of structural proteins in the treated animals could be indicative of



ongoing or incipient repair and healing processes taking effect in the treated group that contributed to the reported resolution of cardiac cell damage. Six months after infarction, there was an indication of post-ischemic conditioning and cytoprotection, as evidenced by the presence of HSP proteins in the treated group (Figure 6). HSP was not detected in any other group, and its detection in the treated group is a consequence of metoprolol administration (44). This is relevant because HSP overexpression attenuates myocardial apoptosis (45,46), and it confirms the activation of cytoprotective processes months after CRT+BB treatment initiation.

The results from the biomarkers used confirm an improved prognosis for the treated animals and support the investigational and interventional opportunity offered by TFMP proteomic profiling post-MI. This was in line with a decline in TnT levels in the treated animals, whereas chronic troponin leak resulting from the death of cardiomyocytes persisted in the infarcted, untreated animals. By having less cell death characterized as a smaller troponin leak, these data suggest that treatment with CRT+BB gradually attenuated cell death in the treated group. The observed increase in ADRB1 levels in the treated group and its decrease in the infarcted animals tracks with reports of increasing  $\beta$ -AR expression after the administration of metoprolol (47,48) and provides further evidence of the long-term cellular effects of metoprolol administration. This observation might suggest that chronic  $\beta$ 1-blockade is associated with recirculation of ADRB1 receptors to the cardiomyocyte surface as the levels of ischemic stressors decline and the surviving cardiomyocyte recovers, possibly via a negative feedback loop. The lower levels of ADRB2 in both infarcted groups are in agreement with published data proposing that most protective adrenergic signaling is mediated via  $\beta$ 2-receptors and Gi signaling. This explains the observed decreased  $\beta$ -AR expression along with lowered sensitivity in the aftermath of an MI (49). Furthermore, impaired intracellular  $\text{Ca}^{2+}$  handling in the failing heart has been ascribed to either a decreased expression of SERCA2a or a shift in the interaction between phospholamban and SR  $\text{Ca}^{2+}$ -ATPase activity (50,51). Additionally, in the failing heart, there is a corresponding increase in SR  $\text{Ca}^{2+}$  ATPase activity with increasing cAMP concentrations (51). This perhaps accounts for the observed cAMP increase in our infarcted animals compared with the control animals. Because metoprolol treatment restores cAMP-dependent inotropic effects independent of  $\beta$ -AR (52), this might explain the observed higher levels of cAMP in the treated animals than in the other groups.

The elevated epinephrine and norepinephrine levels in our infarcted group animals compared with the control animals are in line with expectations in the acute phase of an MI but highlight the ensuing cellular derangement chronically post-MI. Finally, the observed elevation of GRK2 levels underscores the heart's decreased contractile function by the blunting of procontractile signaling of the  $\beta$ -ARs (53).

The composite of these biomarker evaluations and the proteomic profiling of the TFMPs showed that treatment with CRT+BB resulted in improvement in outcome. Using pathway and functional analyses, the proteomic profile of TFMPs coupled the detection of diverse signaling mediators with temporal occurrence to disease status and allowed the prediction of outcome in the post-MI setting. Most importantly, the observed TFMP proteomic profile provided information of additive value to what was obtained by analysis of 8 current biomarkers in our chronic ischemic cardiomyopathy model.

This study focused on chronic ischemic cardiomyopathy in a porcine model of ischemic cardiomyopathy and did not examine the utility of the TPMP proteomic profile in the acute phase. Additionally, in our study, MI was induced by use of a collagen plug and therefore might have missed prelude molecular and cellular information that preceded the incidence of an MI. This, however, does not minimize the demonstration of the utility of TFMP protein content as a cellular methodology to be used to further our understanding of signaling after an MI. These results may not be completely generalizable, but the wealth of information obtained from this study suggests that a follow-on translational study examining the utility of profiling TFMPs in the acute phase is warranted as a next step. Furthermore, given the amount of information obtained from the proteomic profile of TFMPs, it would be interesting to determine whether profiling of the entire MP population would provide additional information. Another necessary next step in this line of inquiry must involve quantitative methods to explore levels of candidate proteins. Furthermore, it would be important to establish relevant flow cytometry thresholds of TFMP counts that would yield levels of putative proteins that would allow for assessment in clinical settings.

## CONCLUSIONS

The composite of the findings of this study is in agreement with previous studies and clinical observations that treatment with CRT+BB after an MI leads to better outcomes. More importantly, our findings, while confirming the heterogeneity of TFMP

protein content, also demonstrate that proteomic profiling of TFMPs from both the infarcted and non-infarcted pigs captured the diversity of the protein contents between and within groups temporally. Changes in the identified proteins within and between groups corresponded to relevant changes in molecular function and reflected the physiological status of the host. Spatially, the contents of the TFMPs displayed a variety of proteins and provided additional information on multiple entities supplemental to what we obtained from assessing 8 of the current cardiac biomarkers. Additionally, for both infarcted groups, there was a noticeable time difference in the detected proteins that predictably reflected active, ongoing cellular activities. Therefore, results of this study support recommending TFMP protein content profiling prospectively as a viable investigative methodology for chronic ischemic cardiomyopathy that could help improve our understanding of  $\beta$ AR signaling after an MI. The ability to dynamically capture active signaling pathways instead of tracking the presence or absence of a single molecular entity, as typified by the current group of biomarkers, would provide pertinent answers to questions about  $\beta$ AR signaling pathways post-MI and in heart failure.

**ACKNOWLEDGMENTS** The authors would like to express their gratitude to Jane Chu, Mahfuz Khan, Irena Brandt, and Kayla Jackson for their contributions in sample and data generation for this study.

**ADDRESS FOR CORRESPONDENCE:** Dr. David S. Feldman, Division of Cardiology, University of Cincinnati Medical Center, 234 Goodman Street, Cincinnati, Ohio 45221. E-mail: [feldmads@ucmail.uc.edu](mailto:feldmads@ucmail.uc.edu).

## PERSPECTIVES

**COMPETENCY IN MEDICAL KNOWLEDGE:** Current models of post-MI signaling involve small animals with monitoring for a few hours to days. Usually, only a few proteins are assessed, which does not adequately depict the pathophysiology in humans. TFMP proteomic profiling after an MI enables observation of both spatial and temporal events in multiple signaling mechanisms in a long-term mini-swine model. Thus, a dynamic evaluation of active signaling pathways using TFMP proteomic profiling would be a valuable source of molecular markers to investigate  $\beta$ AR signaling post-MI.

**TRANSLATIONAL OUTLOOK:** A chronic animal model, 6 months post-MI, might more closely emulate human disease and provide greater clinical translation to the human condition of the long-term consequences of an MI. In addition to spatial signaling (membrane to the nucleus), this study assessed chronic changes in signaling longitudinally, rather than at a single time point, using the proteomic profile of TFMPs. Thus, we demonstrated that time and intracellular or spatial signaling impact the observed outward phenotype of pathological remodeling after an MI within and between groups.

## REFERENCES

1. Liaudet L, Rosenblatt-Velin N. Role of innate immunity in cardiac inflammation after myocardial infarction. *Front Biosci (Schol Ed)* 2013;5:86-104.
2. Boateng S, Sanborn T. Acute myocardial infarction. *Dis Mon* 2013;59:83-96.
3. Vilahur G, Juan-Babot O, Peña E, Oñate B, Casaní L, Badimon L. Molecular and cellular mechanisms involved in cardiac remodeling after acute myocardial infarction. *J Mol Cell Cardiol* 2011;50:522-33.
4. Maack C, Elter T, Böhm M. Beta-blocker treatment of chronic heart failure: comparison of carvedilol and metoprolol. *Congest Heart Fail* 2003;9:263-70.
5. Shin J, Johnson JA. Beta-blocker pharmacogenetics in heart failure. *Heart Fail Rev* 2010;15:187-96.
6. Lalani GG, Birgersdotter-Green U. Cardiac resynchronization therapy in patients with chronic heart failure. *Heart* 2015;101:1008-14.
7. Mookadam F, Moustafa SE. Prevention of late postmyocardial infarction left ventricular remodeling: an update. *Curr Heart Fail Rep* 2009;6:245-53.
8. Combes V, Simon AC, Grau GE, et al. In vitro generation of endothelial microparticles and possible prothrombotic activity in patients with lupus anticoagulant. *J Clin Invest* 1999;104:93-102.
9. Martinez MC, Tual-Chalot S, Leonetti D, Andriantsitohaina R. Microparticles: targets and tools in cardiovascular disease. *Trends Pharmacol Sci* 2011;32:659-65.
10. Morel O, Toti F, Freyssinet JM. Markers of thrombotic disease: procoagulant microparticles [in French]. *Ann Pharm Fr* 2007;65:75-84.
11. Owens AP 3<sup>rd</sup>, Mackman N. Microparticles in hemostasis and thrombosis. *Circ Res* 2011;108:1284-97.
12. Martinez MC, Andriantsitohaina R. Microparticles in angiogenesis: therapeutic potential. *Circ Res* 2011;109:110-9.
13. Puddu P, Puddu GM, Cravero E, Muscari S, Muscari A. The involvement of circulating microparticles in inflammation, coagulation and cardiovascular diseases. *Can J Cardiol* 2010;26:140-5.
14. Simpson RJ, Jensen SS, Lim JW. Proteomic profiling of exosomes: current perspectives. *Proteomics* 2008;8:4083-99.
15. Zwaal RF, Schroit AJ. Pathophysiologic implications of membrane phospholipid asymmetry in blood cells. *Blood* 1997;89:1121-32.
16. Dadu RT, Nambi V, Ballantyne CM. Developing and assessing cardiovascular biomarkers. *Transl Res* 2012;159:265-76.
17. Morel OF, Ohlmann PF, Morel NF, et al. Microparticles and cardiovascular disease. *Arch Mal Coeur Vaiss* 2005;98:226-35.
18. Shantsila E, Kamphuisen PW, Lip GY. Circulating microparticles in cardiovascular disease: implications for atherogenesis and atherothrombosis. *J Thromb Haemost* 2010;8:2358-68.
19. Tushuizen ME, Diamant M, Sturk AF, Nieuwland R. Cell-derived microparticles in the pathogenesis of cardiovascular disease: friend or foe? *Arterioscler Thromb Vasc Biol* 2011;31:4-9.
20. Viera AJ, Mooberry M, Key NS, et al. Microparticles in cardiovascular disease pathophysiology and outcomes. *J Am Soc Hypertens* 2012;6:243-52.

21. Bakouboula BF, Morel OF, Faure AF, et al. Procoagulant membrane microparticles correlate with the severity of pulmonary arterial hypertension. *Am J Respir Crit Care Med* 2008;177:536-43.
22. Housden BE, Perrimon N. Spatial and temporal organization of signaling pathways. *Trends Biochem Sci* 2014;39:457-64.
23. Cui J, Li J, Mathison M, et al. A clinically relevant large-animal model for evaluation of tissue-engineered cardiac surgical patch materials. *Cardiovasc Revasc Med* 2005;6:113-20.
24. Nishijima Y, Sridhar A, Viatchenko-Karpinski S, et al. Chronic cardiac resynchronization therapy and reverse ventricular remodeling in a model of nonischemic cardiomyopathy. *Life Sci* 2007;81:1152-9.
25. Wikstrand J. MERIT-HF: description of the trial. *Basic Res Cardiol* 2000;95 Suppl 1:190-7.
26. Pathan M, Keerthikumar S, Ang CS, et al. FunRich: An open access standalone functional enrichment and interaction network analysis tool. *Proteomics* 2015;15:2597-601.
27. FunRich: Functional Enrichment Analysis Tool. Available at: <http://funrich.org/index.html>. Accessed April 1, 2016.
28. Park HJ, Zhang Y, Georgescu SP, Johnson KL, Kong D, Galper JB. Human umbilical vein endothelial cells and human dermal microvascular endothelial cells offer new insights into the relationship between lipid metabolism and angiogenesis. *Stem Cell Rev* 2006;2:93-102.
29. Hauser S, Jung F, Pietzsch J. Human endothelial cell models in biomaterial research. *Trends Biotechnol* 2017;35:265-77.
30. Onat D, Brillon D, Colombo PC, Schmidt AM. Human vascular endothelial cells: a model system for studying vascular inflammation in diabetes and atherosclerosis. *Curr Diab Rep* 2011;11:193-202.
31. Barrese V, Tagliatela M. New advances in beta-blocker therapy in heart failure. *Front Physiol* 2013;4:323.
32. Prakash A, Markham A. Metoprolol: a review of its use in chronic heart failure. *Drugs* 2000;60:647-78.
33. Talman V, Ruskoaho H. Cardiac fibrosis in myocardial infarction—from repair and remodeling to regeneration. *Cell Tissue Res* 2016;365:563-81.
34. Piek A, de Boer RA, Silljé HH. The fibrosis-cell death axis in heart failure. *Heart Fail Rev* 2016;21:199-211.
35. Ghasemi O, Ma Y, Lindsey ML, Jin YF. Using systems biology approaches to understand cardiac inflammation and extracellular matrix remodeling in the setting of myocardial infarction. *Wiley Interdiscip Rev Syst Biol Med* 2014;6:77-91.
36. Kong P, Christia P, Frangogiannis NG. The pathogenesis of cardiac fibrosis. *Cell Mol Life Sci* 2014;71:549-74.
37. Karpinski L, Witkowska M. Postinfarction cardiac remodeling: clinical consequences [in Polish]. *Przegl Lek* 2009;66:380-3.
38. Kumar SR, Masood R, Spannuth WA, et al. The receptor tyrosine kinase EphB4 is overexpressed in ovarian cancer, provides survival signals and predicts poor outcome. *Br J Cancer* 2007;96:1083-91.
39. Kishimoto I, Tokudome T, Horio T, Garbers DL, Nakao K, Kangawa K. Natriuretic peptide signaling via guanylyl cyclase (GC)-A: an endogenous protective mechanism of the heart. *Curr Cardiol Rev* 2009;5:45-51.
40. Li Y, Kishimoto I, Saito Y, et al. Guanylyl cyclase-A inhibits angiotensin II type 1A receptor-mediated cardiac remodeling, an endogenous protective mechanism in the heart. *Circulation* 2002;106:1722-8.
41. Nakanishi M, Saito Y, Kishimoto I, et al. Role of natriuretic peptide receptor guanylyl cyclase-A in myocardial infarction evaluated using genetically engineered mice. *Hypertension* 2005;46:441-7.
42. George I, Sabbah HN, Xu K, Wang N, Wang J.  $\beta$ -adrenergic receptor blockade reduces endoplasmic reticulum stress and normalizes calcium handling in a coronary embolization model of heart failure in canines. *Cardiovasc Res* 2011;91:447-55.
43. Mao Y, Tokudome T, Otani K, Kishimoto I, Miyazato M, Kangawa K. Excessive sympathoactivation and deteriorated heart function after myocardial infarction in male ghrelin knockout mice. *Endocrinology* 2013;154:1854-63.
44. Tzoporis J, Rizos IK, Toumpoulis I, Salpeas V, Izhar S, Parker TG. The induction of Hsp70 by beta blockade in the human aorta during coronary artery bypass grafting (CABG) or replacement of an ascending thoracic aortic aneurysm (ATAA) is associated with less apoptosis. *Can J Cardiol* 2013; Suppl:S141.
45. Nylandsted J, Jäättelä M, Hoffmann EK, Pedersen SF. Heat shock protein 70 inhibits shrinkage-induced programmed cell death via mechanisms independent of effects on cell volume-regulatory membrane transport proteins. *Pflugers Arch* 2004;449:175-85.
46. Suzuki K, Sawa Y, Kagisaki K, et al. Reduction in myocardial apoptosis associated with over-expression of heat shock protein 70. *Basic Res Cardiol* 2000;95:397-403.
47. Sharma V, Parsons H, Allard MF, McNeill JH. Metoprolol increases the expression of beta(3)-adrenoceptors in the diabetic heart: effects on nitric oxide signaling and forkhead transcription factor-3. *Eur J Pharmacol* 2008;595:44-51.
48. Najafi A, Sequeira V, Kuster DW, van der Velden J.  $\beta$ -adrenergic receptor signalling and its functional consequences in the diseased heart. *Eur J Clin Invest* 2016;46:362-74.
49. Bernstein D, Fajardo G, Zhao M. The role of beta-adrenergic receptors in heart failure: differential regulation of cardiotoxicity and cardioprotection. *Prog Pediatr Cardiol* 2011;31:35-8.
50. Roe AT, Frisk M, Louch WE. Targeting cardiomyocyte  $Ca^{2+}$  homeostasis in heart failure. *Curr Pharm Des* 2015;21:431-48.
51. Schmidt U, Hajjar RJ, Kim CS, Lebeche D, Doye AA, Gwathmey JK. Human heart failure: cAMP stimulation of SR  $Ca^{2+}$ -ATPase activity and phosphorylation level of phospholamban. *Am J Physiol* 1999;277 Pt 2:H474-80.
52. Böhm M, Deutsch HJ, Hartmann D, Rosée KL, Stäblein A. Improvement of postreceptor events by metoprolol treatment in patients with chronic heart failure. *J Am Coll Cardiol* 1997;30:992-6.
53. Cannavo A, Liccardo D, Koch WJ. Targeting cardiac  $\beta$ -adrenergic signaling via GRK2 inhibition for heart failure therapy. *Front Physiol* 2013;4:264.

---

**KEY WORDS**  $\beta$ AR signaling, chronic ischemic cardiomyopathy, matrix signaling, myocardial infarction, tissue factor-bearing microparticles, Yucatan mini swine

---

**APPENDIX** For expanded results, please see the online version of this article.